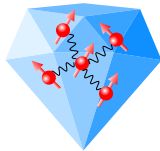
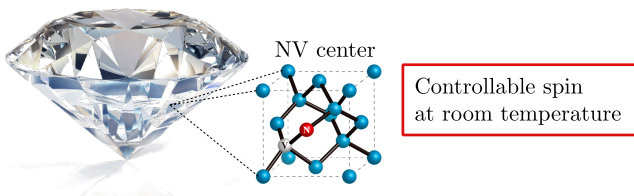


Cross-relaxation in dense ensembles of NV centers and application to magnetometry

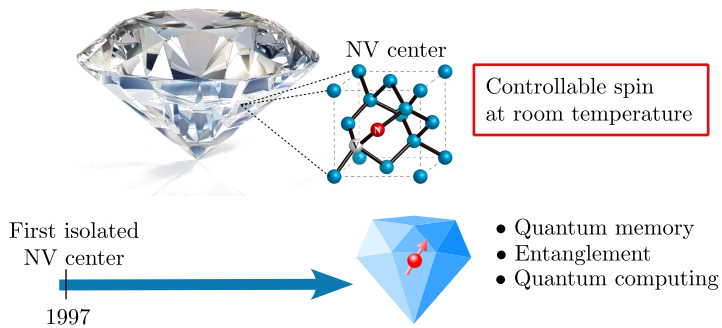
Clément Pellet-Mary PhD Defense



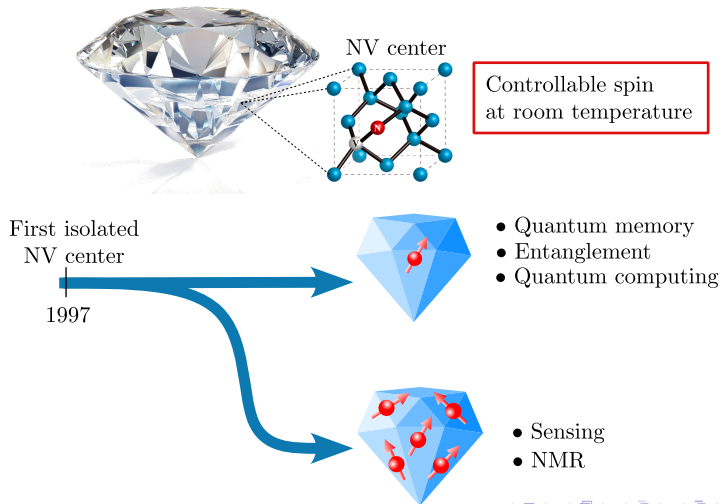
Context of my PhD



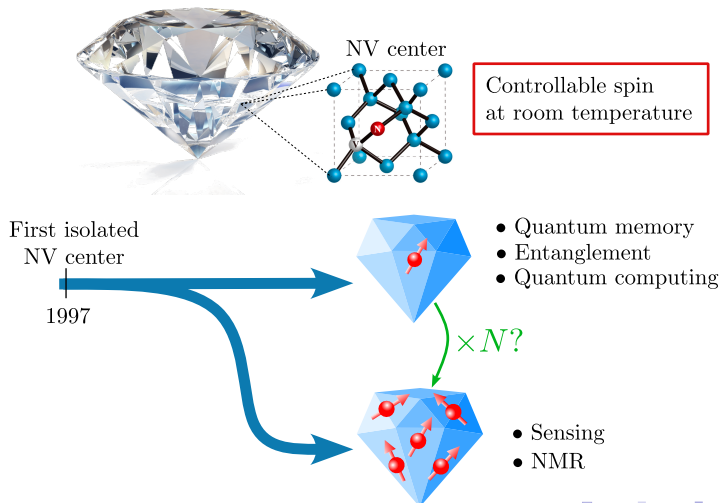
Context of my PhD



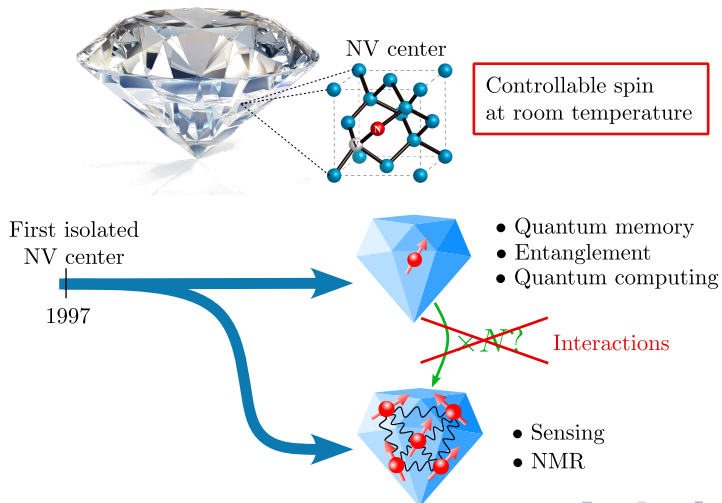
Context of my PhD



Context of my PhD



Context of my PhD



Outline

Sensing with quantum mechanics

NV center spin properties

Low field depolarization magnetometry (LFDM)

Depolarization mechanisms in dense NV ensemble

Outline

Sensing with quantum mechanics

NV center spin properties

Low field depolarization magnetometry (LFDM)

Depolarization mechanisms in dense NV ensemble

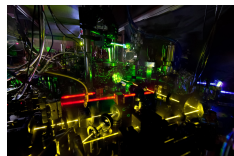
Quantum sensing and metrology

Quantum metrology:

Using quantum* properties to create more sensitive measurement protocols.

* quantum \equiv discrete energy levels

Time measurement



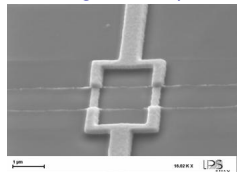
Atomic clock

Medical imaging



MRI

Magnetometry



SQUIDs

Key properties of magnetometers

Sensitivity [T/ $\sqrt{\text{Hz}}$]:

Minimum magnetic field value detectable with a signal-to-noise ratio of 1 within 1 second.

$$|\vec{B}|$$

1 T 1 mT 1 μT



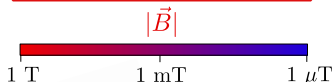
Magnetic source

Magnetometer

Key properties of magnetometers

Sensitivity [T/ $\sqrt{\text{Hz}}$]:

Minimum magnetic field value detectable with a signal-to-noise ratio of 1 within 1 second.



Magnetic source

Magnetometer

$$\xrightarrow{l_{\text{source}}}$$

$$\xrightarrow{l_{\text{sensing}}}$$

Optimum spatial resolution (imaging):

$$l_{\text{sensing}} \leq l_{\text{source}}$$

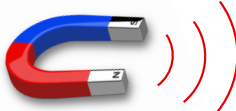
Key properties of magnetometers

Sensitivity [T/ $\sqrt{\text{Hz}}$]:

Minimum magnetic field value detectable with a signal-to-noise ratio of 1 within 1 second.

$$|\vec{B}|$$

1 T 1 mT 1 μT



Magnetic source

$$l_{\text{source}}$$

Magnetometer

$$l_{\text{sensing}}$$

Optimum spatial resolution (imaging):

$$l_{\text{sensing}} \leq l_{\text{source}}$$

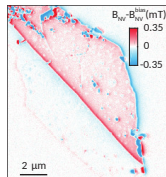
Magnetoencephalography



$$|\vec{B}| \sim 10 \text{ fT}$$

$$l \sim 1 \text{ cm}$$

2D materials magnetism

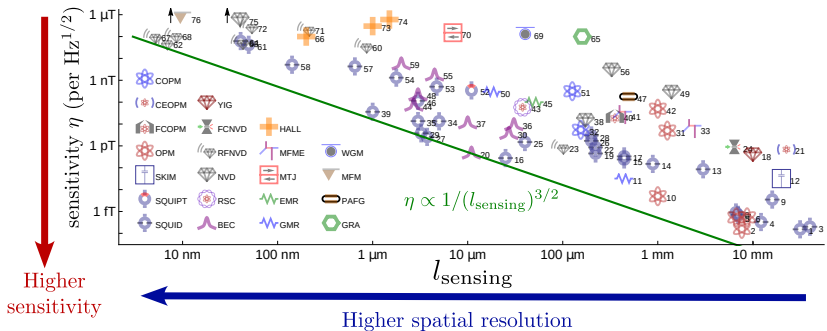


$$|\vec{B}| \sim 100 \mu\text{T}$$

$$l \sim 50 \text{ nm}$$

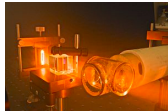
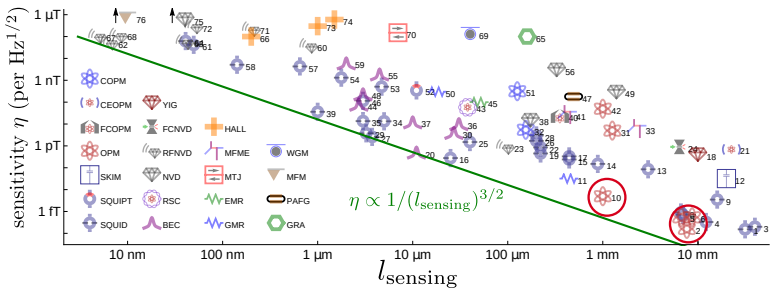
Thiel, L. et al (2019). Science, 364(6444), 973-976.

Sate of the art magnetometers



Mitchell, M. W., & Alvarez, S. P. (2020). *Reviews of Modern Physics*, 92(2), 021001

Sate of the art magnetometers



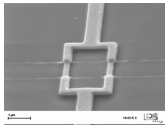
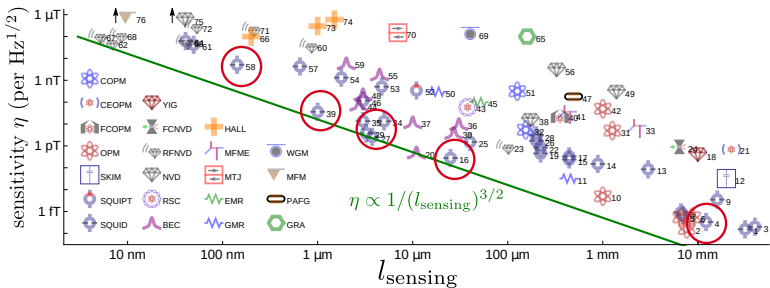
Optically pumped magnetometers (OPM)

✓ Very high sensitivity

✗ Limited in size

Mitchell, M. W., & Alvarez, S. P. (2020). *Reviews of Modern Physics*, 92(2), 021001

State of the art magnetometers

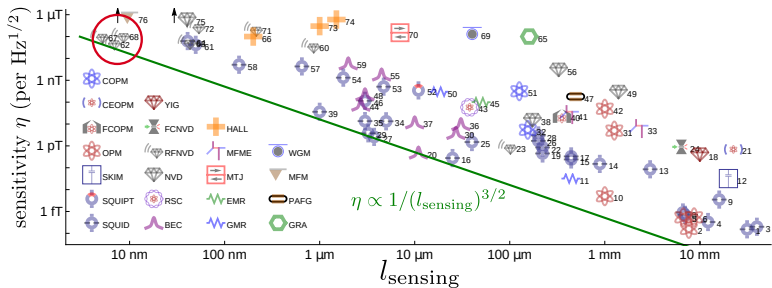


Superconducting quantum interference device (SQUID)

- ✓ High versatility, mature technology
- ✗ Requires cryogenic temperatures

Mitchell, M. W., & Alvarez, S. P. (2020). *Reviews of Modern Physics*, 92(2), 021001

State of the art magnetometers

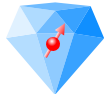
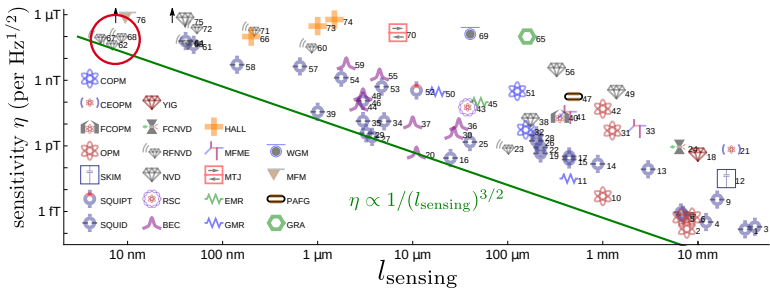


(Single) NV center

- nm resolution
- Room temperature

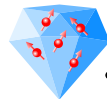
Mitchell, M. W., & Alvarez, S. P. (2020). *Reviews of Modern Physics*, 92(2), 021001

State of the art magnetometers



(Single) NV center

- nm resolution
- Room temperature

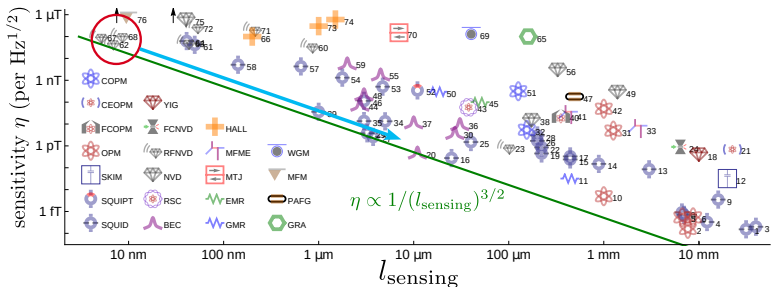


NV ensemble

- μm resolution
- Room temperature
- Higher sensitivity

Mitchell, M. W., & Alvarez, S. P. (2020). Reviews of Modern Physics, 92(2), 021001

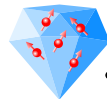
State of the art magnetometers



(Single) NV center

- nm resolution
- Room temperature

$$\eta \propto 1/\sqrt{N} \propto 1/\sqrt{V}$$

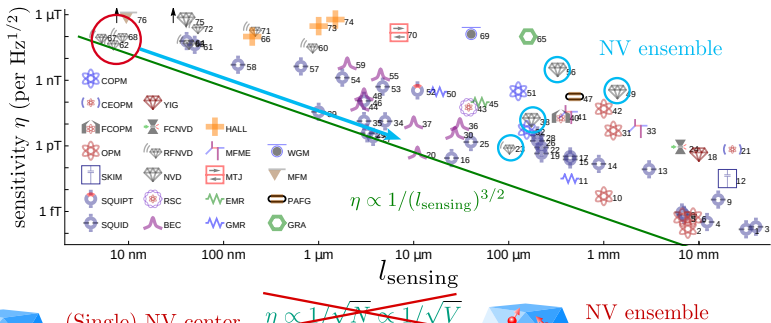


NV ensemble

- μm resolution
- Room temperature
- Higher sensitivity

Mitchell, M. W., & Alvarez, S. P. (2020). *Reviews of Modern Physics*, 92(2), 021001

State of the art magnetometers



(Single) NV center

- nm resolution
- Room temperature

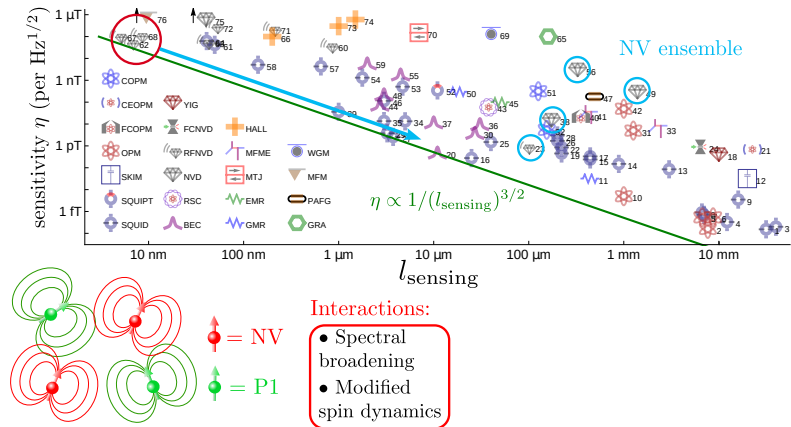
Interactions

NV ensemble

- μm resolution
- Room temperature
- Higher sensitivity

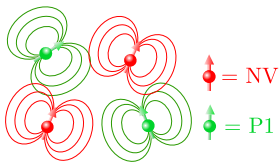
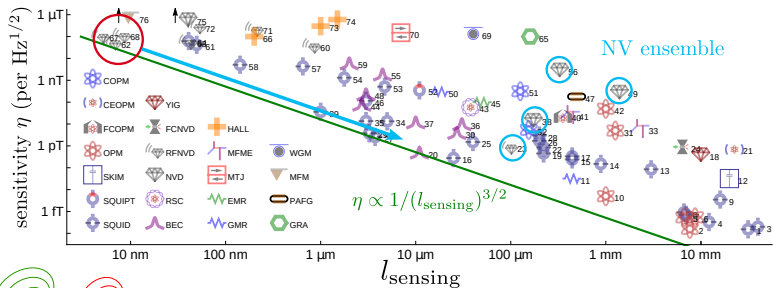
Mitchell, M. W., & Alvarez, S. P. (2020). Reviews of Modern Physics, 92(2), 021001

State of the art magnetometers



Mitchell, M. W., & Alvarez, S. P. (2020). *Reviews of Modern Physics*, 92(2), 021001

State of the art magnetometers



Interactions:

- Spectral broadening
- Modified spin dynamics

Solutions:

- Decoupling interactions (Hamiltonian engineering)
- Exploiting interactions

Mitchell, M. W., & Alvarez, S. P. (2020). *Reviews of Modern Physics*, 92(2), 021001

Outline

Sensing with quantum mechanics

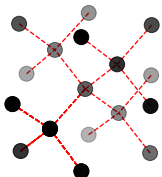
NV center spin properties

Low field depolarization magnetometry (LFDM)

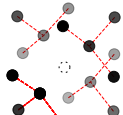
Depolarization mechanisms in dense NV ensemble

Colored centers in diamond

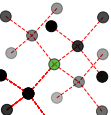
Diamond crystal lattice



Point-like defects



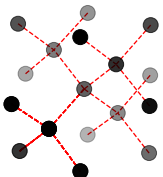
Vacancy



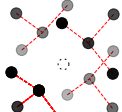
Substitution

Colored centers in diamond

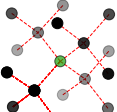
Diamond crystal lattice



Point-like defects

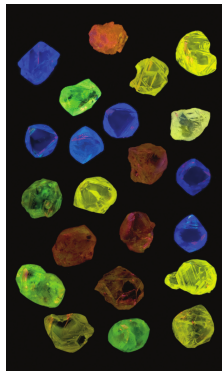
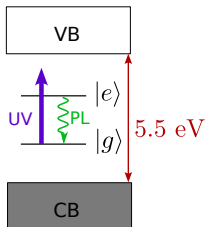


Vacancy



Substitution

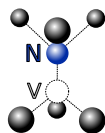
Colored center fluorescence



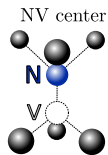
Natural diamonds fluorescence under UV light

Synthetic diamond and NV centers

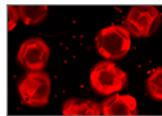
NV center



Synthetic diamond and NV centers



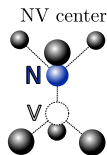
High Pressure High Temperature
(HPHT)



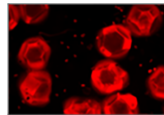
Adamas 15/150 μm

$[\text{NV}] \approx 3 \text{ ppm}$

Synthetic diamond and NV centers



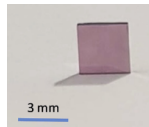
High Pressure High Temperature
(HPHT)



Adamas 15/150 μm

$[\text{NV}] \approx 3 \text{ ppm}$

Chemical Vapour Deposition
(CVD)

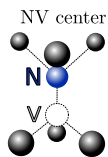


IRCP-LSPM

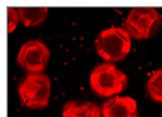
$[\text{NV}] \approx 4.5 \text{ ppm}$

Tallaire, A., et al (2020). Carbon, 170, 421-429.

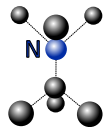
Synthetic diamond and NV centers



High Pressure High Temperature
(HPHT)



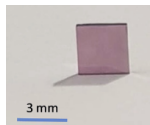
N_s (P1 center)



Adamas 15/150 μm

$[\text{NV}] \approx 3 \text{ ppm}$
 $[\text{P1}] \approx 100 \text{ ppm}$

Chemical Vapour Deposition
(CVD)



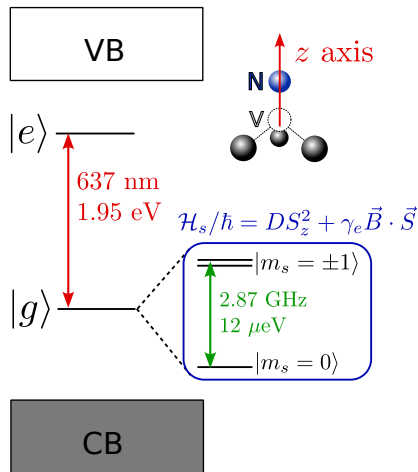
IRCP-LSPM

$[\text{NV}] \approx 4.5 \text{ ppm}$
 $[\text{P1}] \approx 25 \text{ ppm}$

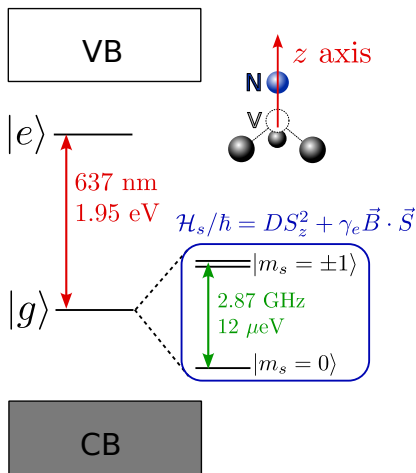
Tallaire, A., et al (2020). Carbon, 170, 421-429.

Edmonds, A. M. et al (2021). Materials for Quantum Technology, 1(2), 025001.

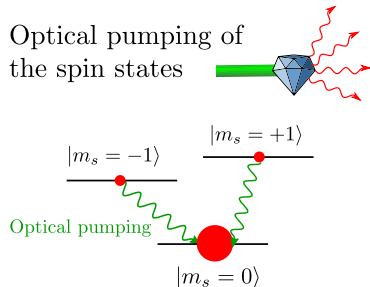
The NV center energy levels



The NV center energy levels

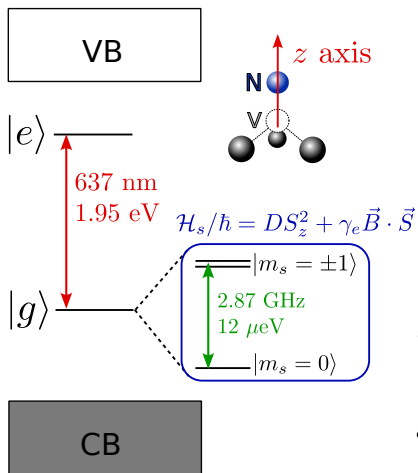


Optical pumping of the spin states

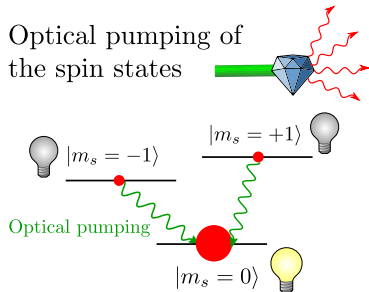


- Population accumulation in the $|0\rangle$ state
 - ↳ Initialization of the spin state

The NV center energy levels

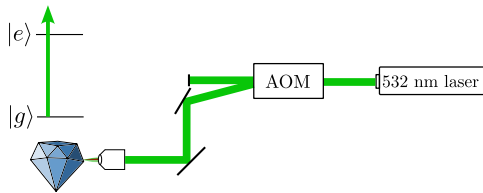


Optical pumping of the spin states

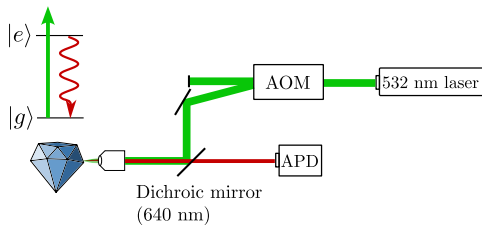


- Population accumulation in the $|0\rangle$ state
 - ↳ Initialization of the spin state
- $|0\rangle$ state brighter than $|\pm 1\rangle$ states
 - ↳ Optical readout of the spin state

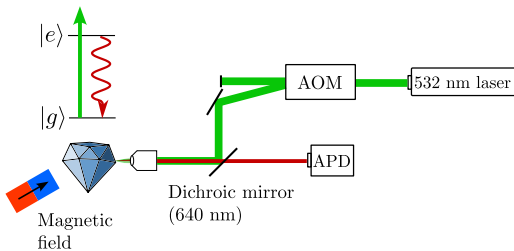
Experimental setup



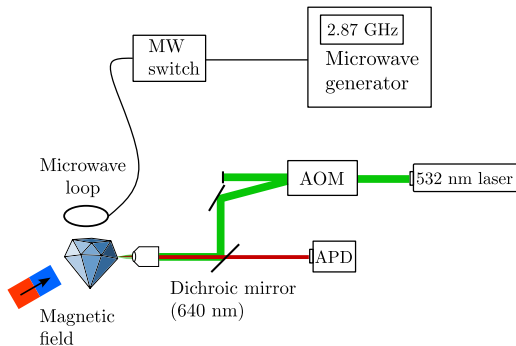
Experimental setup



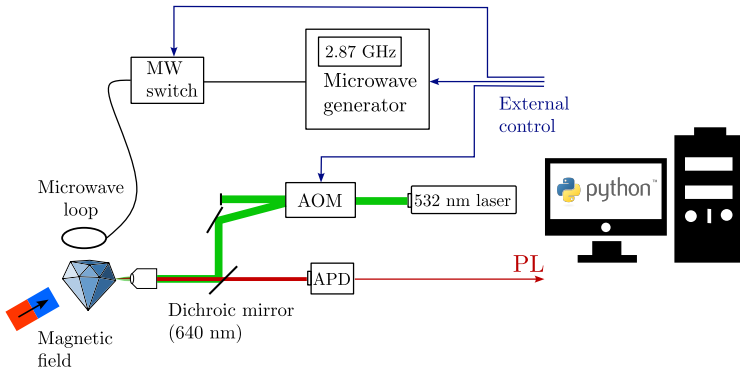
Experimental setup



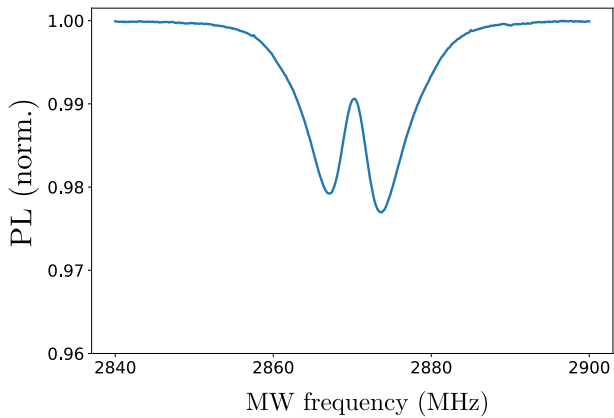
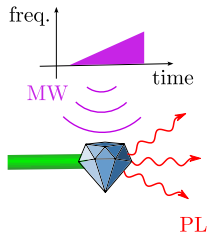
Experimental setup



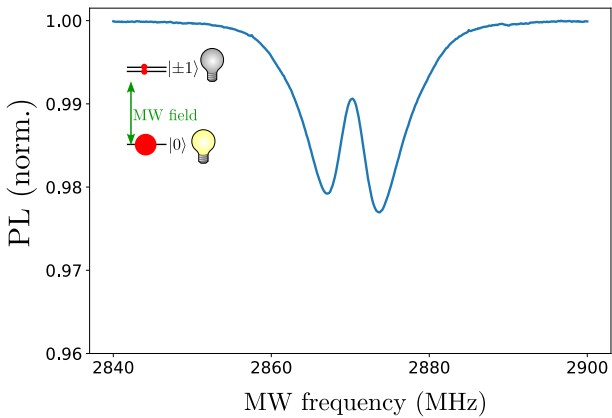
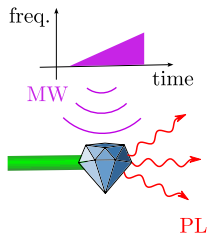
Experimental setup



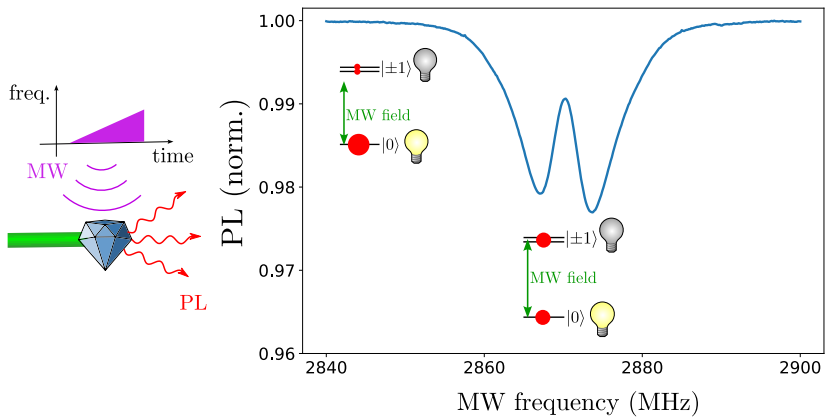
Optically detected magnetic resonance (ODMR)



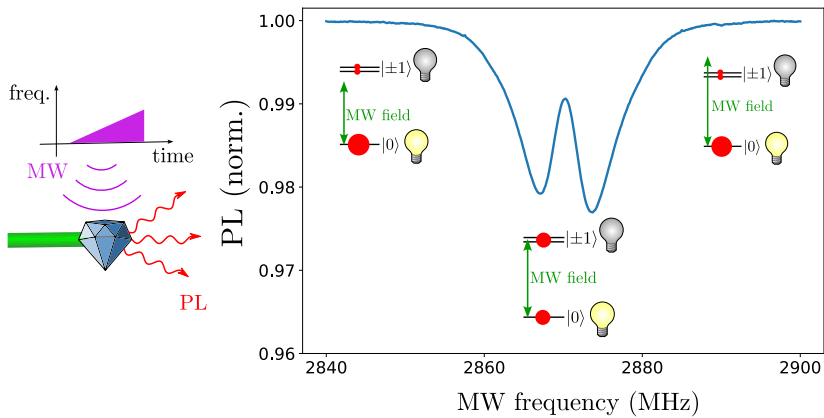
Optically detected magnetic resonance (ODMR)



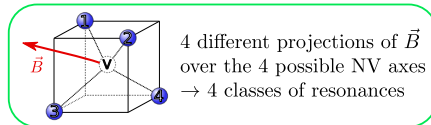
Optically detected magnetic resonance (ODMR)



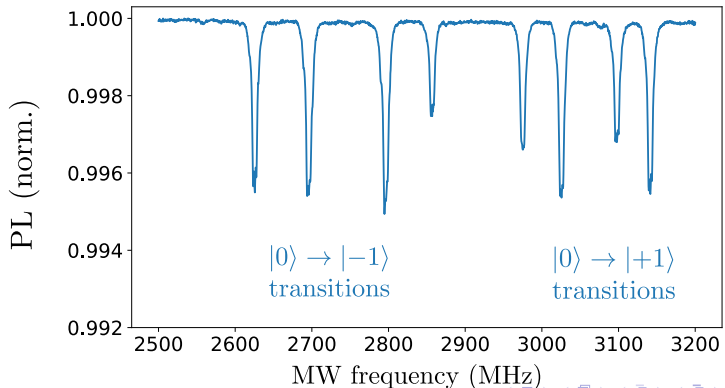
Optically detected magnetic resonance (ODMR)



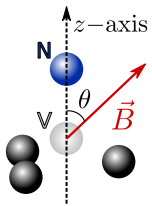
ODMR with NV ensemble: the 4 classes



Position of the 8 lines:
→ 3D reconstruction of \vec{B}



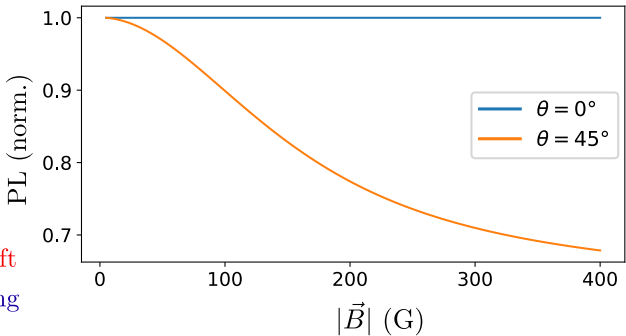
Transverse magnetic field effect



B_{\parallel} = Zeeman shift

B_{\perp} = State mixing

Loss of polarization, PL decrease



Outline

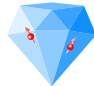
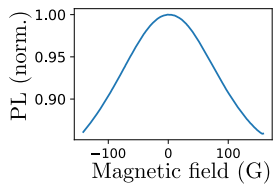
Sensing with quantum mechanics

NV center spin properties

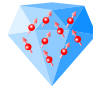
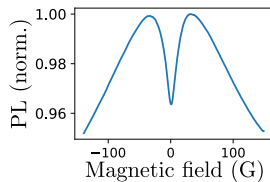
Low field depolarization magnetometry (LFDM)

Depolarization mechanisms in dense NV ensemble

Depolarization of dense NV ensemble at low magnetic field

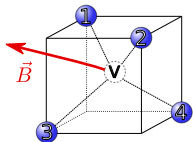


Low NV density
[NV] \leq 100 ppb

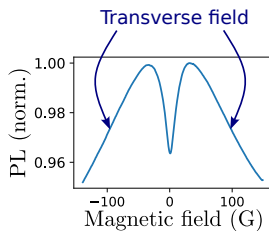
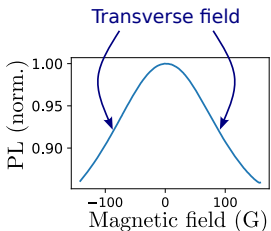


High NV density
[NV] \geq 1 ppm

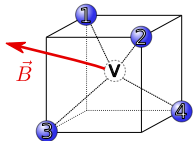
Depolarization of dense NV ensemble at low magnetic field



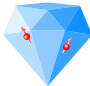
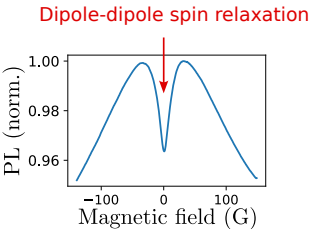
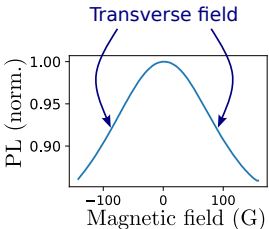
Non-zero transverse magnetic field on all 4 classes



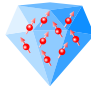
Depolarization of dense NV ensemble at low magnetic field



Non-zero transverse magnetic field on all 4 classes

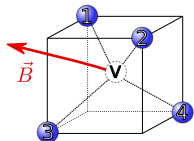


Low NV density
[NV] \leq 100 ppb

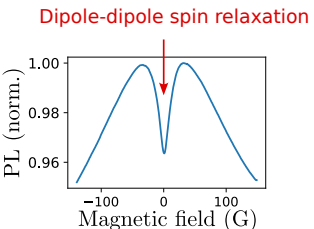
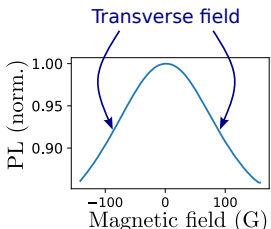


High NV density
[NV] \geq 1 ppm

Depolarization of dense NV ensemble at low magnetic field

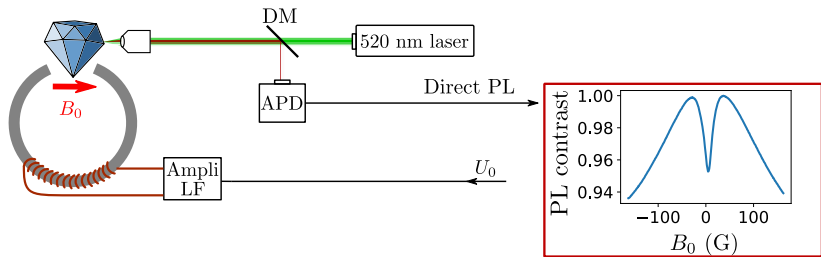


Non-zero transverse magnetic field on all 4 classes

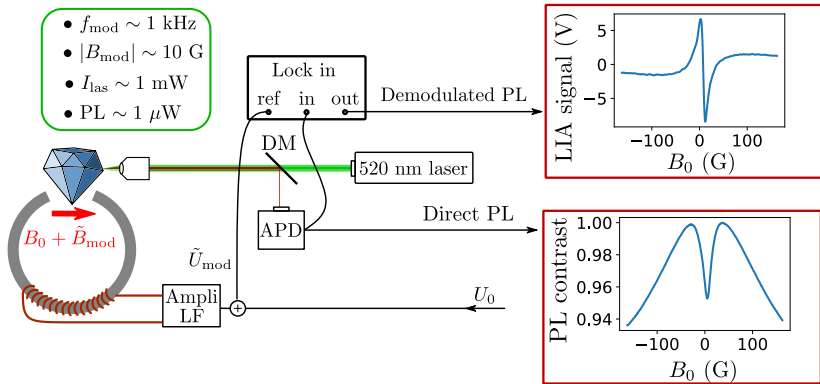


Sharp PL feature → magnetometry

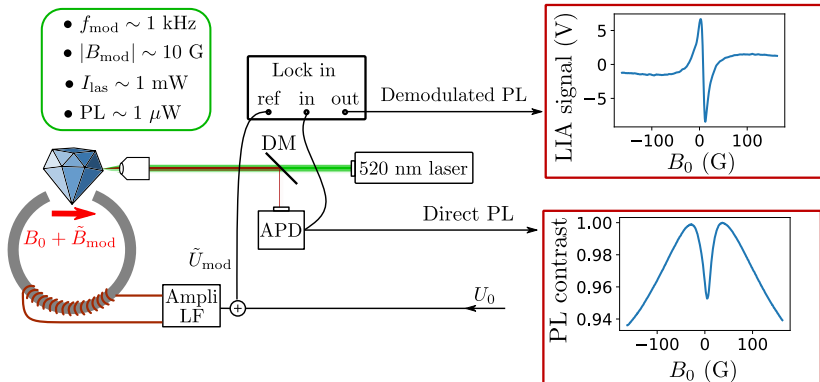
LFDM experimental setup



LFDM experimental setup



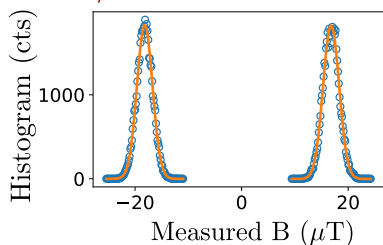
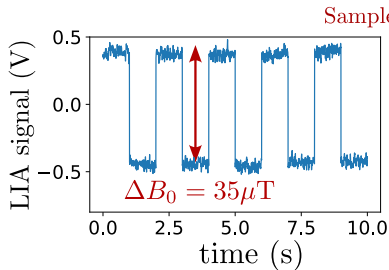
LFDM experimental setup



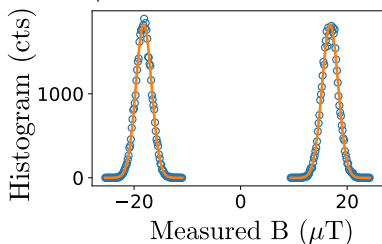
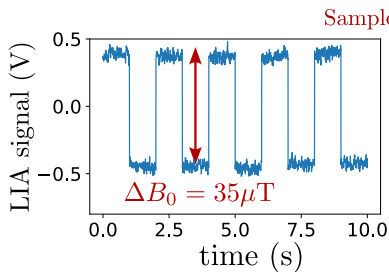
LIA:

- Avoid low frequency noise
- Linear dependance between U_{out} and B_0

Sensitivity of LFDM



Sensitivity of LFDM



Measurement time $\tau = 3 \text{ ms} \quad \sqrt{\langle \delta B^2 \rangle} \approx 1.2 \mu\text{T}$

\rightarrow sensitivity $\eta = \sqrt{2\tau \langle \delta B^2 \rangle} \approx 120 \text{ nT}/\sqrt{\text{Hz}}$

Comparison with the state of the art

Sensitivity comparison

	ODMR [1]	GSLAC [2]	LFDM
η (nT/ $\sqrt{\text{Hz}}$)	0.015	0.3	116

[1] Barry, J. F. [...] Walsworth, R. L (2016). PNAS, 113(49), 14133-14138.

[2] Zheng, H.[...] Budker, D. (2020). Physical Review Applied, 13(4), 044023.

Comparison with the state of the art

Sensitivity comparison

	ODMR [1]	GSLAC [2]	LFDM
η (nT/ $\sqrt{\text{Hz}}$)	0.015	0.3	116
V (μm^3)	$5.2 \cdot 10^6$?	$3.3 \cdot 10^3$
η_v (nT $\mu\text{m}^{3/2}\text{Hz}^{-1/2}$)	34	?	6700

[1] Barry, J. F. [...] Walsworth, R. L (2016). PNAS, 113(49), 14133-14138.

[2] Zheng, H.[...] Budker, D. (2020). Physical Review Applied, 13(4), 044023.

Comparison with the state of the art

Sensitivity comparison

	ODMR [1]	GSLAC [2]	LFDM
η (nT/ $\sqrt{\text{Hz}}$)	0.015	0.3	116
V (μm^3)	$5.2 \cdot 10^6$?	$3.3 \cdot 10^3$
η_v (nT $\mu\text{m}^{3/2}\text{Hz}^{-1/2}$)	34	?	6700

[1] Barry, J. F. [...] Walsworth, R. L (2016). PNAS, 113(49), 14133-14138.

[2] Zheng, H.[...] Budker, D. (2020). Physical Review Applied, 13(4), 044023.

	ODMR	GSLAC	LFDM
Microwave free	✗	✓	✓

Comparison with the state of the art

Sensitivity comparison

	ODMR [1]	GSLAC [2]	LFDM
η (nT/ $\sqrt{\text{Hz}}$)	0.015	0.3	116
V (μm^3)	$5.2 \cdot 10^6$?	$3.3 \cdot 10^3$
η_v (nT $\mu\text{m}^{3/2}\text{Hz}^{-1/2}$)	34	?	6700

[1] Barry, J. F. [...] Walsworth, R. L (2016). PNAS, 113(49), 14133-14138.

[2] Zheng, H.[...] Budker, D. (2020). Physical Review Applied, 13(4), 044023.

	ODMR	GSLAC	LFDM
Microwave free	✗	✓	✓
Low magnetic field (<10 G)	✓	✗	✓

Comparison with the state of the art

Sensitivity comparison

	ODMR [1]	GSLAC [2]	LFDM
η (nT/ $\sqrt{\text{Hz}}$)	0.015	0.3	116
V (μm^3)	$5.2 \cdot 10^6$?	$3.3 \cdot 10^3$
η_v (nT $\mu\text{m}^{3/2}\text{Hz}^{-1/2}$)	34	?	6700

[1] Barry, J. F. [...] Walsworth, R. L (2016). PNAS, 113(49), 14133-14138.

[2] Zheng, H.[...] Budker, D. (2020). Physical Review Applied, 13(4), 044023.

ODMR GSLAC LFDM

Microwave free	✗	✓	✓
Low magnetic field (<10 G)	✓	✗	✓
Robust to T° and B-field inhomogeneities	✗	✗	✓

Comparison with the state of the art

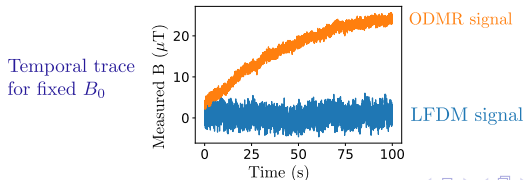
Sensitivity comparison

	ODMR [1]	GSLAC [2]	LFDM
η (nT/ $\sqrt{\text{Hz}}$)	0.015	0.3	116
V (μm^3)	$5.2 \cdot 10^6$?	$3.3 \cdot 10^3$
η_v (nT $\mu\text{m}^{3/2}\text{Hz}^{-1/2}$)	34	?	6700

[1] Barry, J. F. [...] Walsworth, R. L (2016). PNAS, 113(49), 14133-14138.

[2] Zheng, H. [...] Budker, D. (2020). Physical Review Applied, 13(4), 044023.

	ODMR	GSLAC	LFDM
Microwave free	✗	✓	✓
Low magnetic field (<10 G)	✓	✗	✓
Robust to T° and B-field inhomogeneities	✗	✗	✓



Comparison with the state of the art

Sensitivity comparison

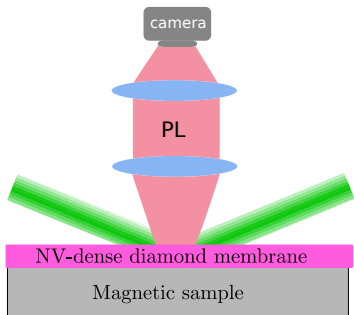
	ODMR [1]	GSLAC [2]	LFDM
η (nT/ $\sqrt{\text{Hz}}$)	0.015	0.3	116
V (μm^3)	$5.2 \cdot 10^6$?	$3.3 \cdot 10^3$
η_v (nT $\mu\text{m}^{3/2}\text{Hz}^{-1/2}$)	34	?	6700

[1] Barry, J. F. [...] Walsworth, R. L (2016). PNAS, 113(49), 14133-14138.

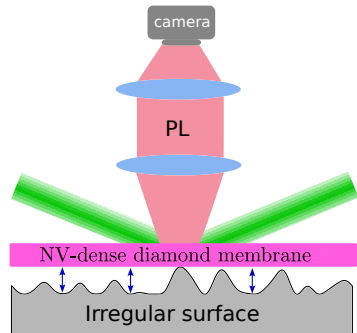
[2] Zheng, H.[...] Budker, D. (2020). Physical Review Applied, 13(4), 044023.

	ODMR	GSLAC	LFDM
Microwave free	✗	✓	✓
Low magnetic field (<10 G)	✓	✗	✓
Robust to T° and B-field inhomogeneities	✗	✗	✓
Orientation free (polycrystalline, powder)	✗	✗	✓

Application: wide-field magnetometry

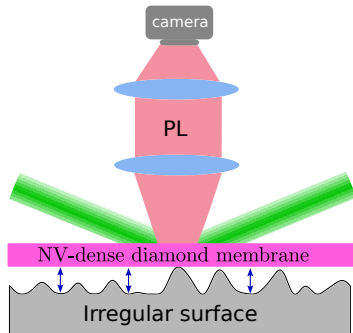


Application: wide-field magnetometry

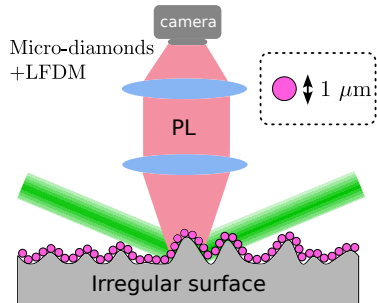


Gaps: loss of spatial resolution

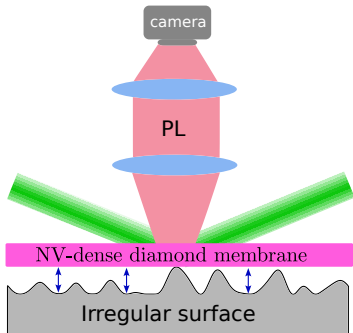
Application: wide-field magnetometry



Gaps: loss of spatial resolution



Application: wide-field magnetometry

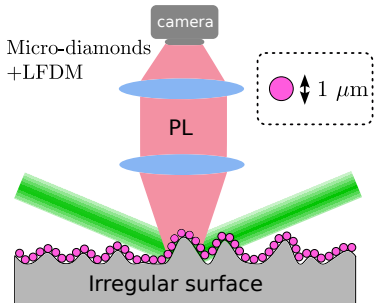


Gaps: loss of spatial resolution

State of the art [1]:

Area normalized sensitivity:
 $\eta_S \approx 20 \mu\text{T} \cdot \mu\text{m}/\sqrt{\text{Hz}}$

[1] Glenn, D. R. [...] Walsworth, R. L. (2017) Geochemistry, Geophysics, Geosystems, 18(8), 3254–3267.



LFDM :

Area normalized sensitivity:
 $\eta_S \approx 6 \mu\text{T} \cdot \mu\text{m}/\sqrt{\text{Hz}}$

Outline

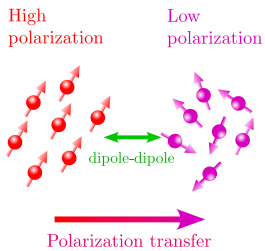
Sensing with quantum mechanics

NV center spin properties

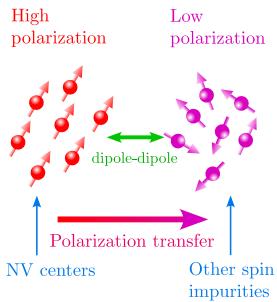
Low field depolarization magnetometry (LFDM)

Depolarization mechanisms in dense NV ensemble

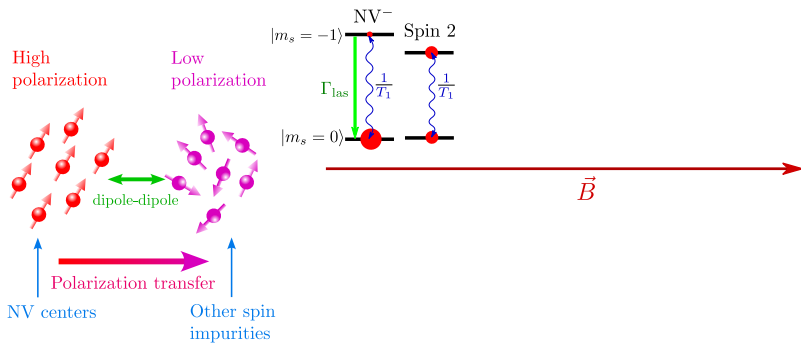
Principle of cross-relaxation with NV centers



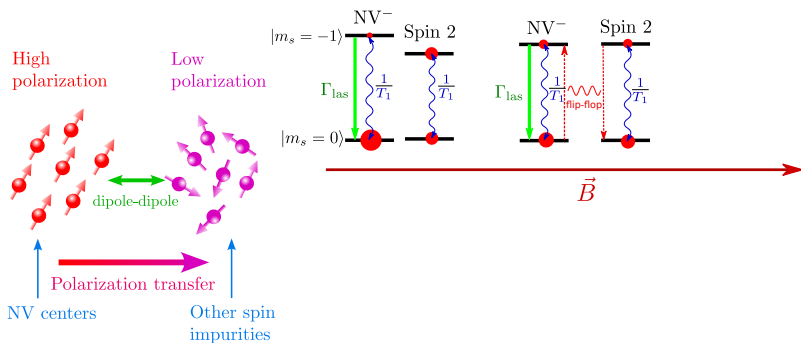
Principle of cross-relaxation with NV centers



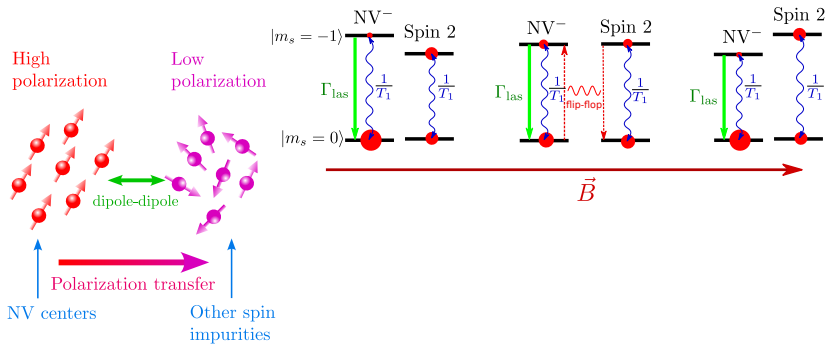
Principle of cross-relaxation with NV centers



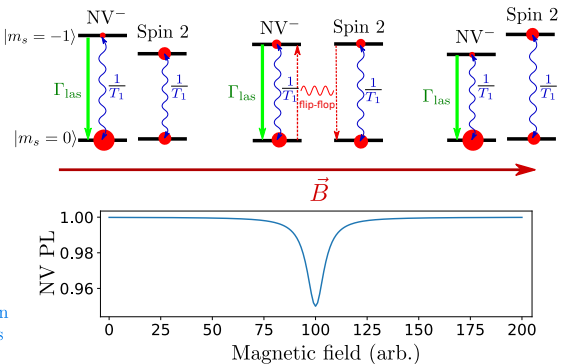
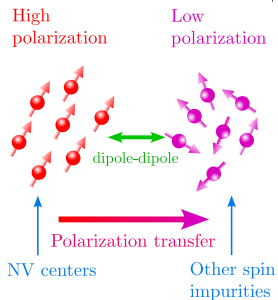
Principle of cross-relaxation with NV centers



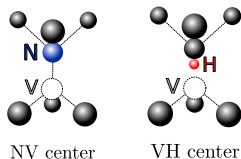
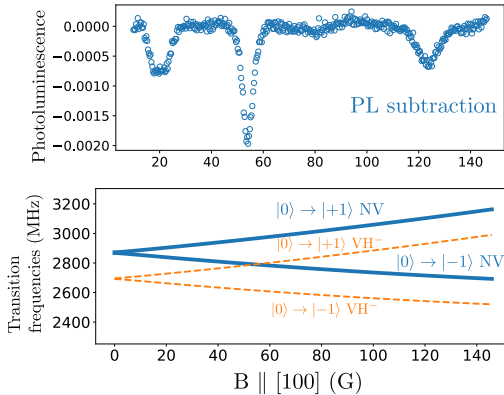
Principle of cross-relaxation with NV centers



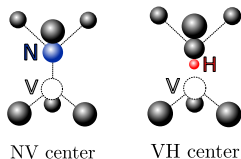
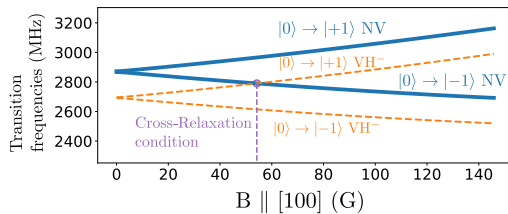
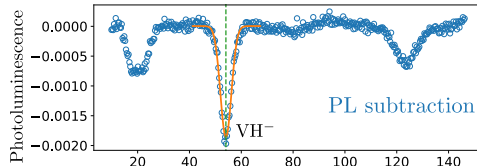
Principle of cross-relaxation with NV centers



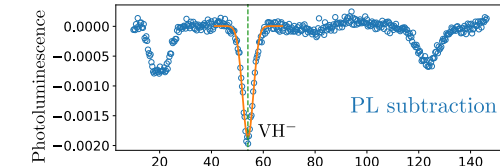
Example: Cross-relaxation between NV centers and VH⁻



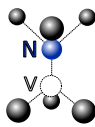
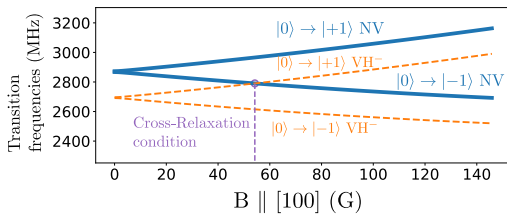
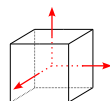
Example: Cross-relaxation between NV centers and VH⁻



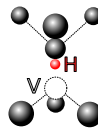
Example: Cross-relaxation between NV centers and VH⁻



$$\vec{B} \parallel \langle 100 \rangle$$

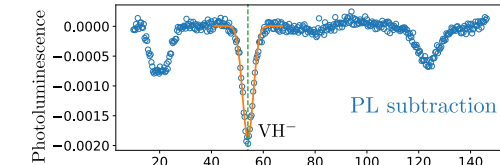


NV center

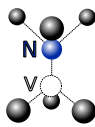
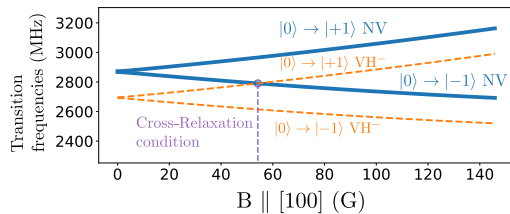
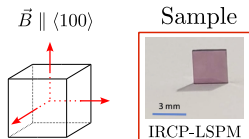


VH center

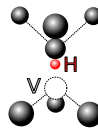
Example: Cross-relaxation between NV centers and VH⁻



$\vec{B} \parallel \langle 100 \rangle$

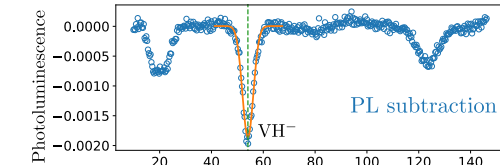


NV center

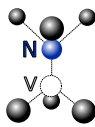
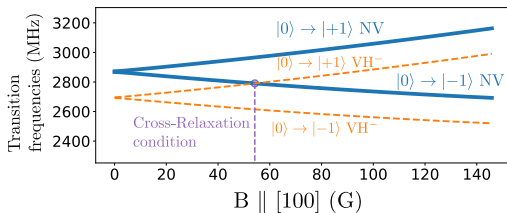
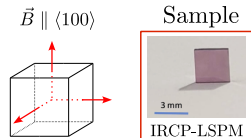


VH center

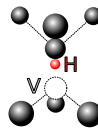
Example: Cross-relaxation between NV centers and VH⁻



$\vec{B} \parallel \langle 100 \rangle$



NV center

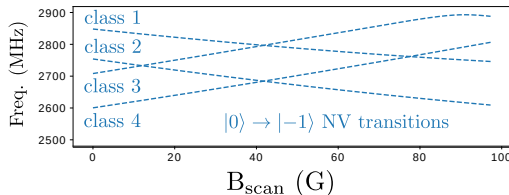


VH center

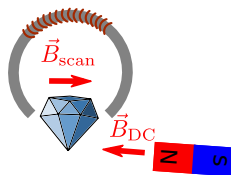
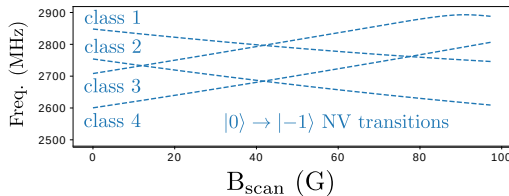
Optical detection of paramagnetic defects in diamond grown by chemical vapor deposition

C. Pellet-Mary, P. Huillery, M. Perdrat, A. Tallaire, and G. Hétet
Phys. Rev. B **103**, L100411 – Published 24 March 2021

Cross-relaxation between NV centers and NV centers

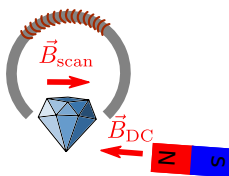
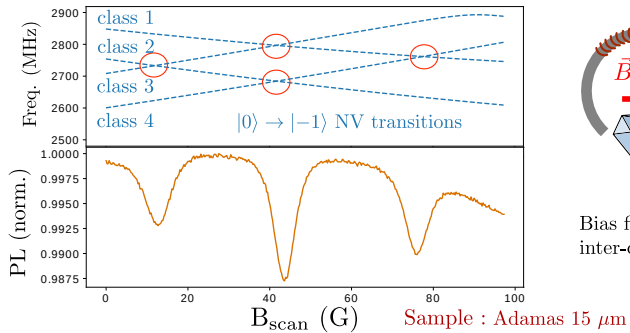


Cross-relaxation between NV centers and NV centers



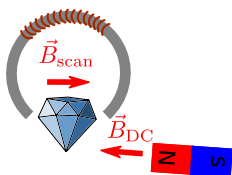
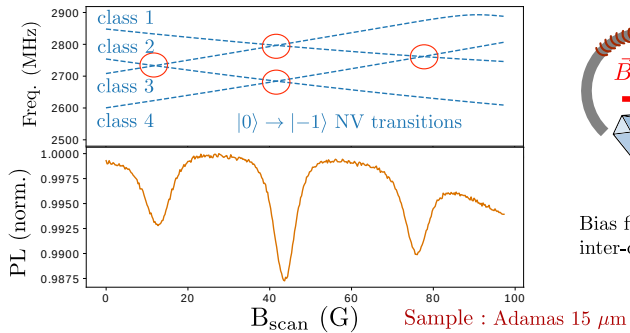
Bias field required to create inter-class resonances

Cross-relaxation between NV centers and NV centers

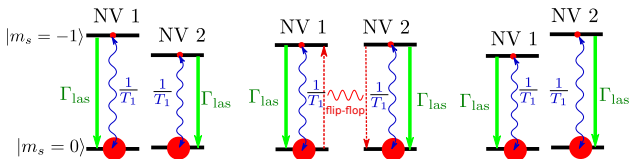


Bias field required to create inter-class resonances

Cross-relaxation between NV centers and NV centers



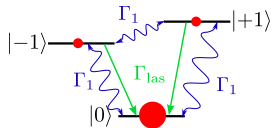
Bias field required to create inter-class resonances



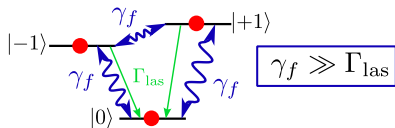
Problem:
no CR for equally polarized spins

Presentation of the fluctuator model

Normal NV

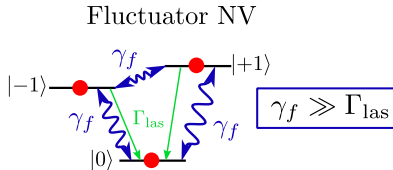
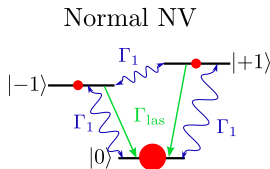


Fluctuator NV



Choi, J. [...] Lukin, M. D. (2017). PRL, 118(9), 093601.

Presentation of the fluctuator model

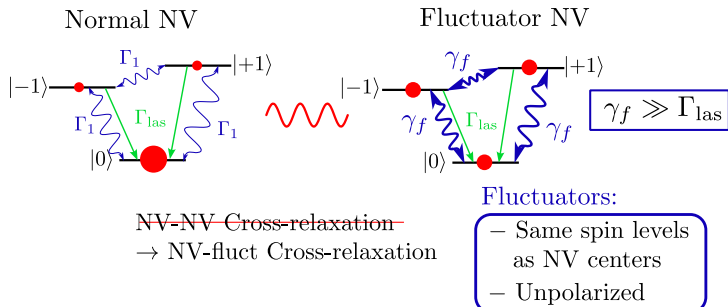


Fluctuators:

- Same spin levels as NV centers
- Unpolarized

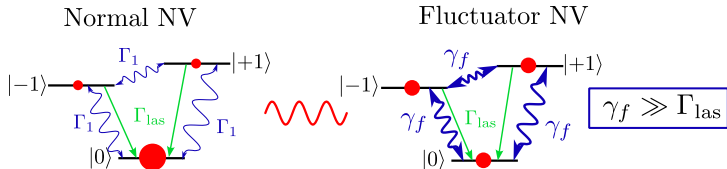
Choi, J. [...] Lukin, M. D. (2017). PRL, 118(9), 093601.

Presentation of the fluctuator model



Choi, J. [...] Lukin, M. D. (2017). PRL, 118(9), 093601.

Presentation of the fluctuator model



~~NV-NV Cross-relaxation~~
→ NV-fluct Cross-relaxation

Fluctuators:

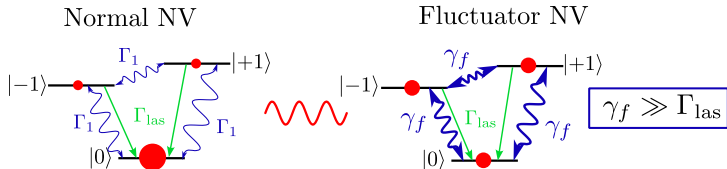
- Same spin levels as NV centers
- Unpolarized

Precedents in:

- P-doped Si
- Solid-state NMR
- FRET

Choi, J. [...] Lukin, M. D. (2017). PRL, 118(9), 093601.

Presentation of the fluctuator model



~~NV-NV Cross-relaxation~~
→ NV-fluct Cross-relaxation

Fluctuators:

- Same spin levels as NV centers
- Unpolarized

Precedents in:

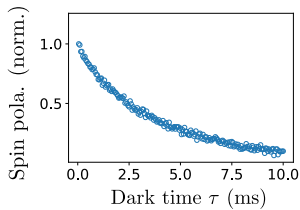
- P-doped Si
- Solid-state NMR
- FRET

Potential microscopic origin:

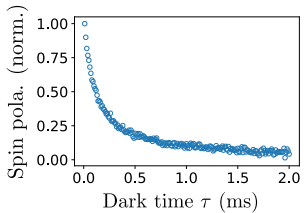
- Charge tunneling
 - Modulation of contact interaction
- Fluctuator = impurity cluster

Choi, J. [...] Lukin, M. D. (2017). PRL, 118(9), 093601.

Stretched exponential decay profile

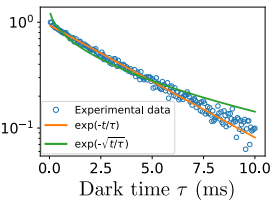
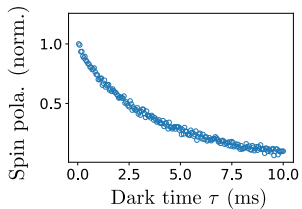


Low NV density
• $T_1 \sim 5$ ms



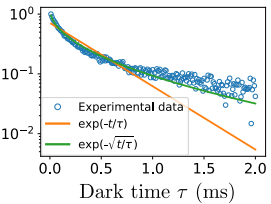
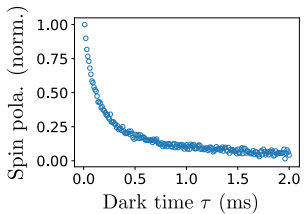
High NV density
• $T_1 \sim 0.5$ ms

Stretched exponential decay profile



Low NV density

- $T_1 \sim 5$ ms
- Exponential profile

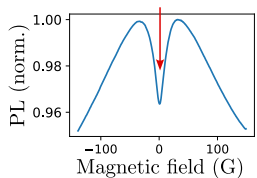


High NV density

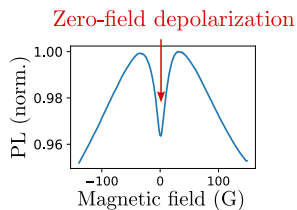
- $T_1 \sim 0.5$ ms
- Stretched exp. profile

Zero field depolarization mechanisms (theory)

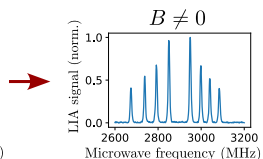
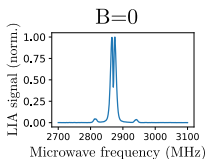
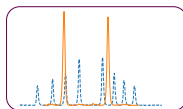
Zero-field depolarization



Zero field depolarization mechanisms (theory)



- 4-classes degeneracy

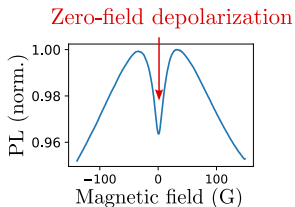


Increased magnetic field

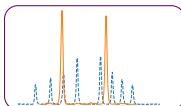
→ lift of the 4 classes degeneracy

→ reduction of spin exchange

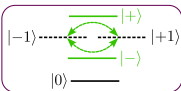
Zero field depolarization mechanisms (theory)



- 4-classes degeneracy



- Eigenbasis change



Spin Hamiltonian dominated
by local \vec{E} -field at low \vec{B} -field

$$|\pm\rangle = \frac{|+1\rangle \pm |-1\rangle}{\sqrt{2}}$$

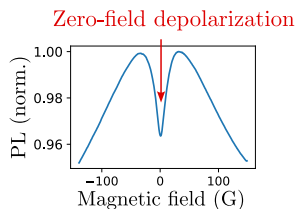
Mittiga, T., [...], Yao, N. Y. (2018). PRL, 121(24), 246402.

New eigenstates in zero-field

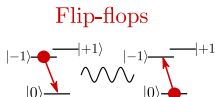
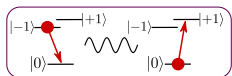
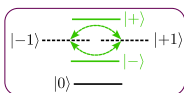
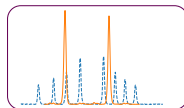
→ new dipole-dipole coupling rates

→ increased depolarization in zero-field

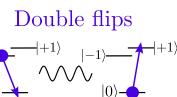
Zero field depolarization mechanisms (theory)



- 4-classes degeneracy
- Eigenbasis change
- Double flips

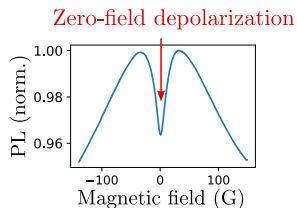


$| -1, 0 \rangle \rightarrow | 0, -1 \rangle$
Always resonant

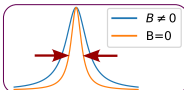
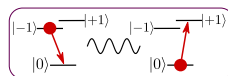
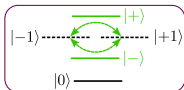
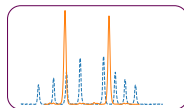


$| -1, 0 \rangle \rightarrow | 0, +1 \rangle$
Only resonant in 0B

Zero field depolarization mechanisms (theory)

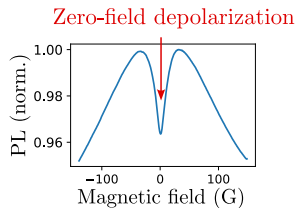


- 4-classes degeneracy
- Eigenbasis change
- Double flips
- T_2^* increase

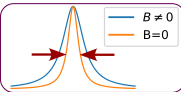
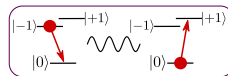
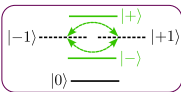
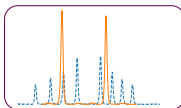


Lower spectral linewidth → Higher coupling rate

Zero field depolarization mechanisms (theory)



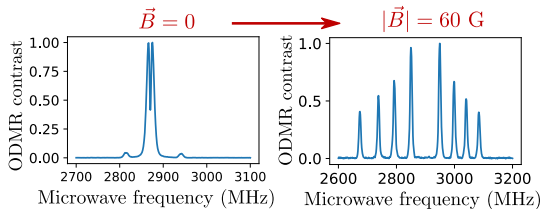
- 4-classes degeneracy
- Eigenbasis change
- Double flips
- T_2^* increase



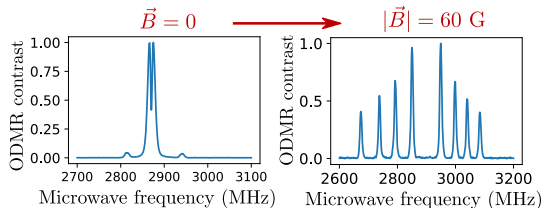
Relative contribution (averaged over all configurations):

4 classes-degeneracy \gg Double-flips > Eigenbasis change $\approx T_2^*$ increase

Experiment: \vec{B} in arbitrary direction

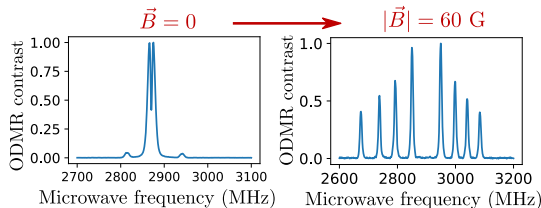


Experiment: \vec{B} in arbitrary direction

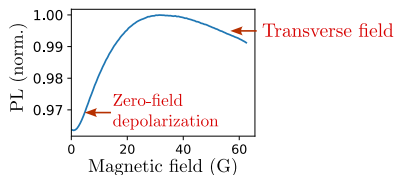


- 4-classes degeneracy
- Eigenbasis change
- Double-flips
- T_2^* change

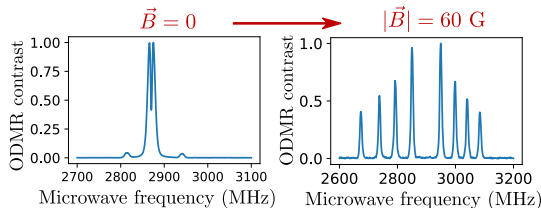
Experiment: \vec{B} in arbitrary direction



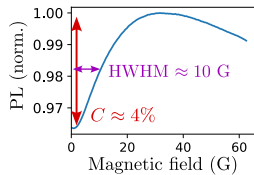
- 4-classes degeneracy
- Eigenbasis change
- Double-flips
- T_2^* change



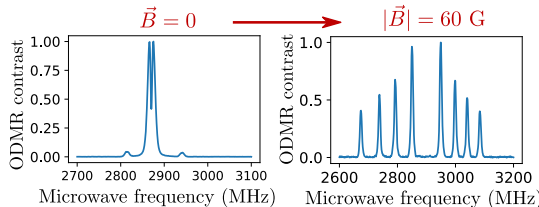
Experiment: \vec{B} in arbitrary direction



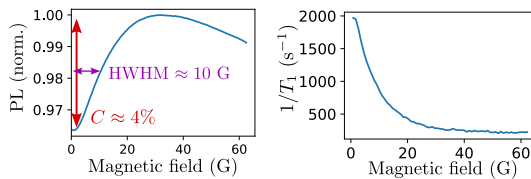
- 4-classes degeneracy
- Eigenbasis change
- Double-flips
- T_2^* change



Experiment: \vec{B} in arbitrary direction

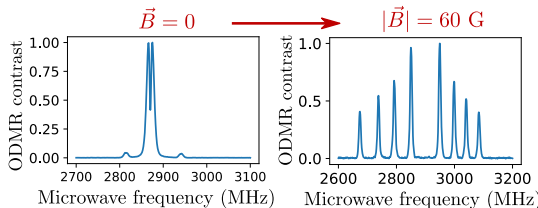


- 4-classes degeneracy
- Eigenbasis change
- Double-flips
- T_2^* change

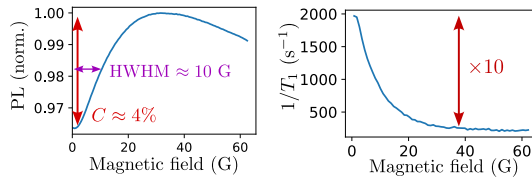


T_1 measured for each magnetic field values

Experiment: \vec{B} in arbitrary direction

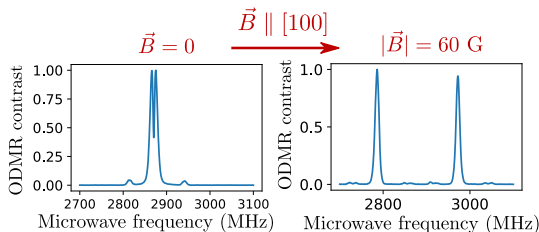


- 4-classes degeneracy
- Eigenbasis change
- Double-flips
- T_2^* change

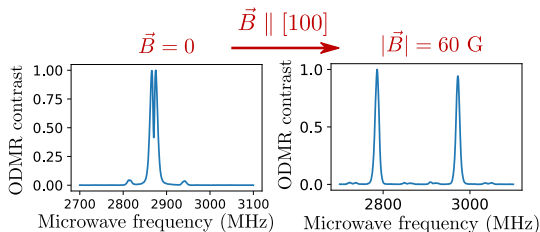


Depolarization increased by $\sim \times 10$ in zero magnetic field

Experiment: $\vec{B} \parallel [100]$

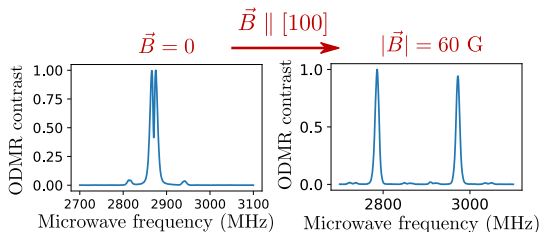


Experiment: $\vec{B} \parallel [100]$

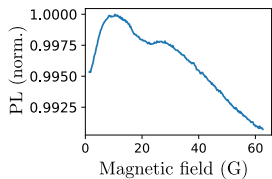


- 4 classes degeneracy
- Eigenbasis change
- Double-flips
- T_2^* change

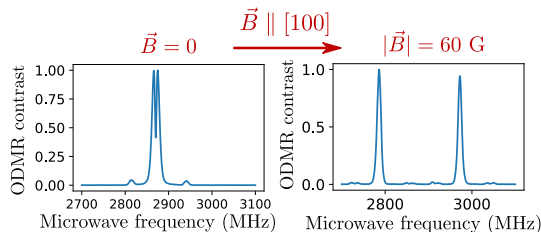
Experiment: $\vec{B} \parallel [100]$



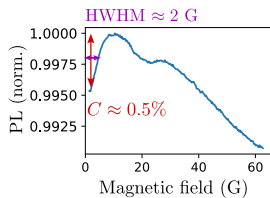
- 4 classes degeneracy
- Eigenbasis change
- Double-flips
- T_2^* change



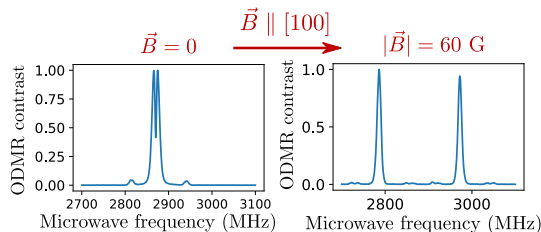
Experiment: $\vec{B} \parallel [100]$



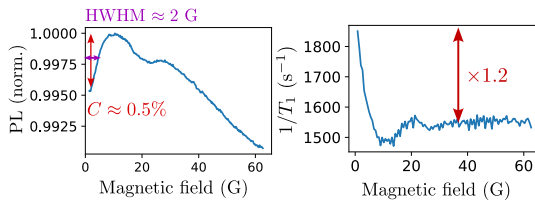
- 4 classes degeneracy
- Eigenbasis change
- Double-flips
- T_2^* change



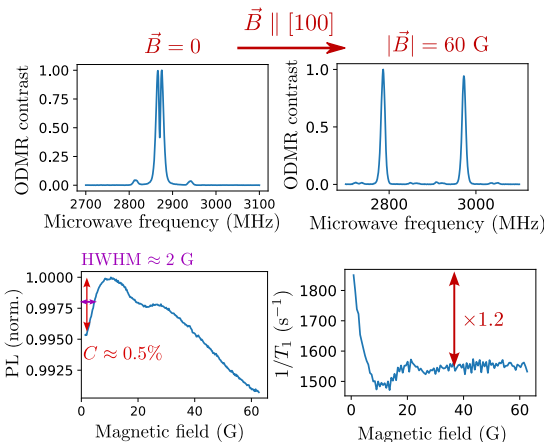
Experiment: $\vec{B} \parallel [100]$



- 4 classes degeneracy
- Eigenbasis change
- Double-flips
- T_2^* change



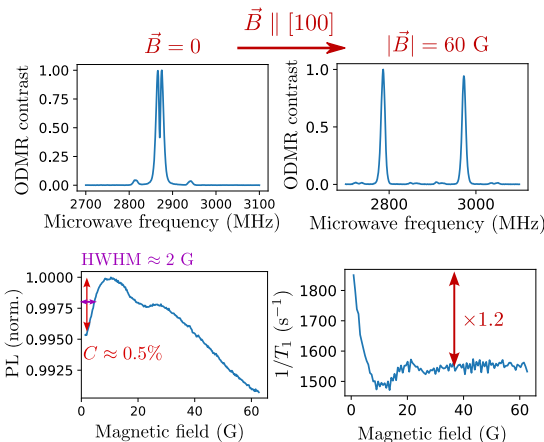
Experiment: $\vec{B} \parallel [100]$



- 4 classes degeneracy
- Eigenbasis change
- Double-flips
- T_2^* change

Depolarization
increased by $\sim \times 1.2$
in zero magnetic field

Experiment: $\vec{B} \parallel [100]$



- 4 classes degeneracy
- Eigenbasis change
- Double-flips
- T_2^* change

Depolarization
increased by $\sim \times 1.2$
in zero magnetic field

4-classes degeneracy dominates low-field depolarization

Sensing with quantum mechanics

NV center spin properties

Low field depolarization magnetometry (LFDM)

Depolarization mechanisms in dense NV ensemble

Cross-relaxations

The fluctuator model

Low field depolarization mechanisms

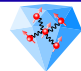
Conclusion

Conclusion

Conclusion

Key points:

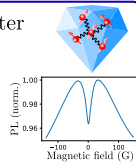
- NV center ensemble are promising room-temperature magnetometer but are partly limited by the interactions between the spins.



Conclusion

Key points:

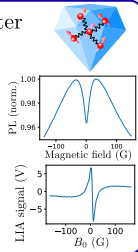
- NV center ensemble are promising room-temperature magnetometer but are partly limited by the interactions between the spins.
- Dipole-dipole interaction in dense ensemble of NV centers causes spin relaxation. The effect is stronger at low magnetic field.



Conclusion

Key points:

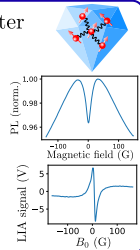
- NV center ensemble are promising room-temperature magnetometer but are partly limited by the interactions between the spins.
- Dipole-dipole interaction in dense ensemble of NV centers causes spin relaxation. The effect is stronger at low magnetic field.
- The low field depolarization effect can be used to create microwave-free and orientation-free magnetometers.



Conclusion

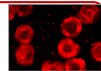
Key points:

- NV center ensemble are promising room-temperature magnetometer but are partly limited by the interactions between the spins.
- Dipole-dipole interaction in dense ensemble of NV centers causes spin relaxation. The effect is stronger at low magnetic field.
- The low field depolarization effect can be used to create microwave-free and orientation-free magnetometers.



Perspectives:

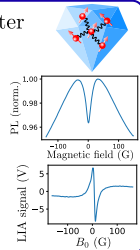
- Further studies on low field depolarization: temperature dependence, material aspects...



Conclusion

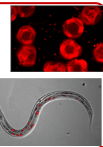
Key points:

- NV center ensemble are promising room-temperature magnetometer but are partly limited by the interactions between the spins.
- Dipole-dipole interaction in dense ensemble of NV centers causes spin relaxation. The effect is stronger at low magnetic field.
- The low field depolarization effect can be used to create microwave-free and orientation-free magnetometers.



Perspectives:

- Further studies on low field depolarization: temperature dependence, material aspects...
- LFDM applications: real-time magnetometry in liquids, background-free fluorescence microscopy, large NV magnetometers...



Acknowledgments

Diamond team

Gabriel Hétet
Maxime Perdriat

Paul Huillery
Tom Delord
Louis Nicolas

IRCP/LSPM

Alexandre Tallaire
Philippe Goldner
Jocelyn Achard
Midrel Ngandeu Ngambo

Nano-optics

Christophe Voisin
Carole Diederichs
Yannick Chassagneux
Emmanuel Baudin
Christos Flytzanis

Antoine Borel
Raouf Amara
Zakaria Said
Marin Tharrault
Pierre-Louis Phélix
Federico Rapisarda

Hadrien Vergnet
Romaric Le Goff
Théo Claude

Direction

Jean-Marc Berroir
Jean-Michel Isac

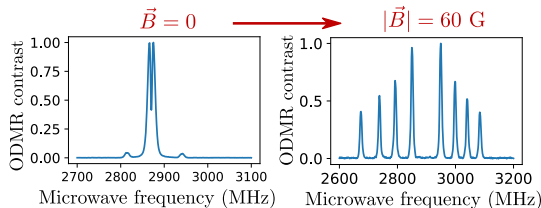
Technical Staff

Pascal Morfin
Arnaud Leclercq
Nabil Garroum
The mechanical workshop
Didier Courtiade and his team

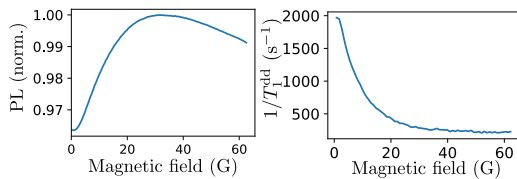
Administrative staff

Olga Hodges
Christine Chambon

Experiment: \vec{B} in arbitrary direction

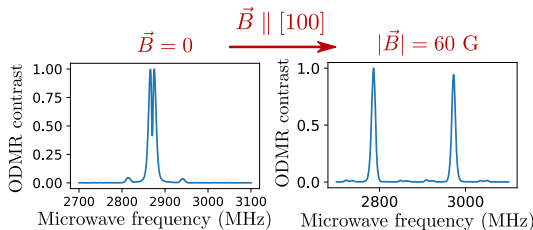


- 4-classes degeneracy
- Eigenbasis change
- Double-flips
- T_2^* change

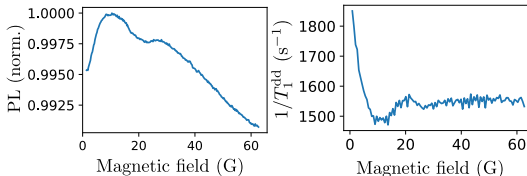


$\Gamma_1(B = 0) \approx 10 \Gamma_1(B \neq 0)$
 $\sim 4\%$ PL contrast
 HWHM ~ 9 G

Experiment: $\vec{B} \parallel [100]$



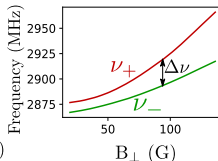
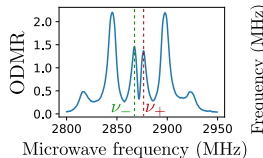
- 4-classes degeneracy
- Eigenbasis change
- Double-flips
- T_2^* change



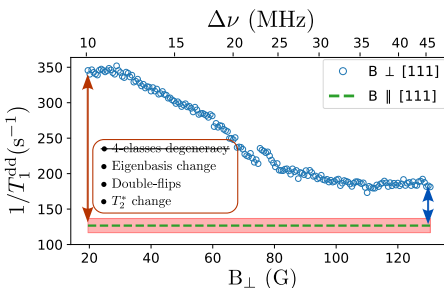
$\Gamma_1(B = 0) \approx 1.2 \Gamma_1(B \neq 0)$
 $\sim 0.5\% \text{ PL contrast}$
 $\text{HWHM} \sim 2 \text{ G}$

Classes degeneracy is the dominant cause
of depolarization at low magnetic field

Experiment: $\vec{B} \perp [111]$



Same eigenbasis :
 $|\pm\rangle = \frac{|+1\rangle \pm |-1\rangle}{\sqrt{2}}$
 for $\vec{B} \perp [111]$ than for $\vec{B} = 0$

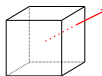


canceling out double flips
 with transverse field

- 4 classes degeneracy
- Eigenbasis change
- Double-flips
- T_2^* change

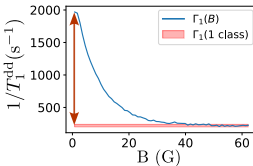
Double flips are the second dominant cause
 of depolarization at low magnetic field

Summary of the experimental observations

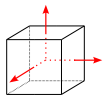


Random \vec{B}

- 4-classes degeneracy
- Eigenbasis change
- Double-flips
- T_2^* change

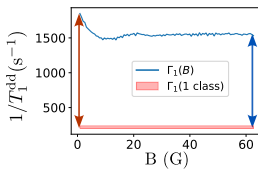


- 4-classes degeneracy
- Eigenbasis change
- Double-flips
- T_2^* change

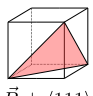


$\vec{B} \parallel \langle 100 \rangle$

- 4-classes degeneracy
- Eigenbasis change
- Double-flips
- T_2^* change

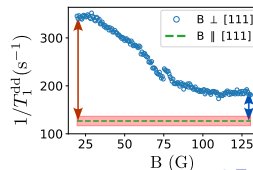


- 4-classes degeneracy
- Eigenbasis change
- Double-flips
- T_2^* change



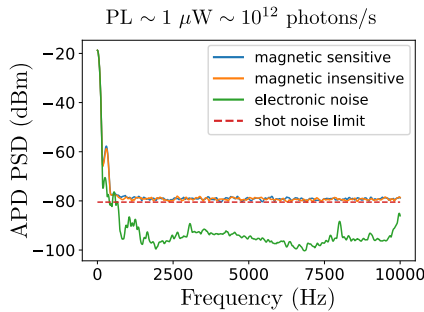
$\vec{B} \perp \langle 111 \rangle$

- 4-classes degeneracy
- Eigenbasis change
- Double-flips
- T_2^* change

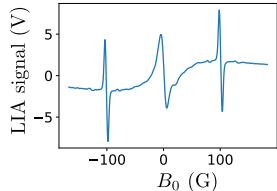
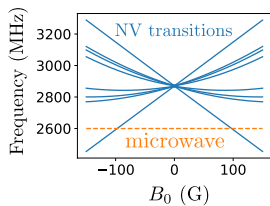
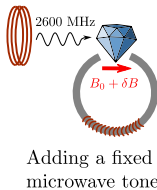


- 4-classes degeneracy
- Eigenbasis change
- Double-flips
- T_2^* change

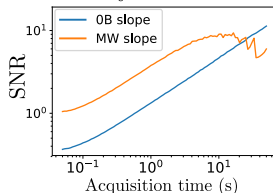
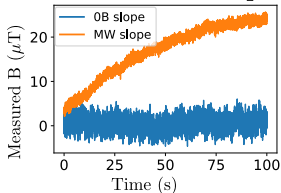
LFDM: shot-noise limit



Comparison with CW ODMR



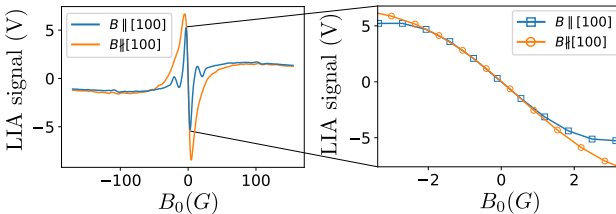
Temporal stability



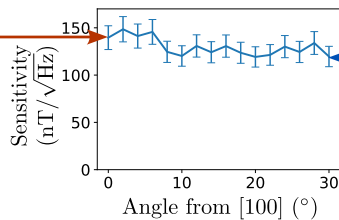
$$\text{MW slope sensitivity: } \eta \approx 40 \text{ nT}/\sqrt{\text{Hz}}$$

$$B=0 \text{ sensitivity: } \eta \approx 120 \text{ nT}/\sqrt{\text{Hz}}$$

Angular sensitivity of LFDM



- 4 classes degeneracy
- Eigenbasis change
- Double-flips
- T_2^* change

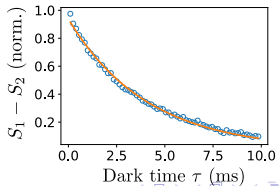
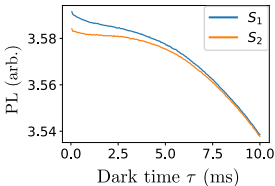
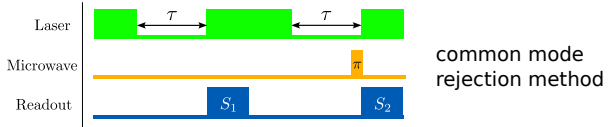
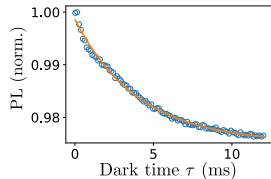
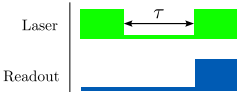


- 4-classes degeneracy
- Eigenbasis change
- Double-flips
- T_2^* change

The 4-classes degeneracy is not the limiting factor of the sensitivity

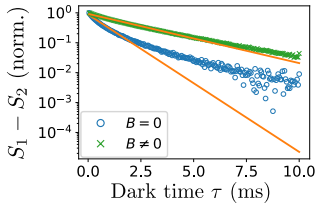
Protocol T1

Basic T1 protocol

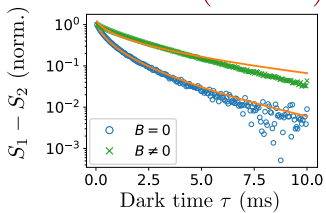


Protocol T1

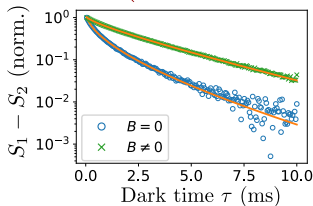
$$f(\tau) = \exp\left(-\tau/T_1^{\text{ph}}\right)$$



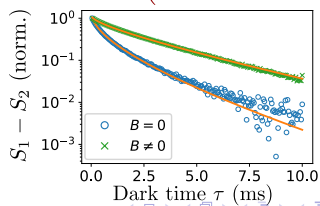
$$f(\tau) = \exp\left(-\sqrt{\tau}/T_1^{\text{dd}}\right)$$



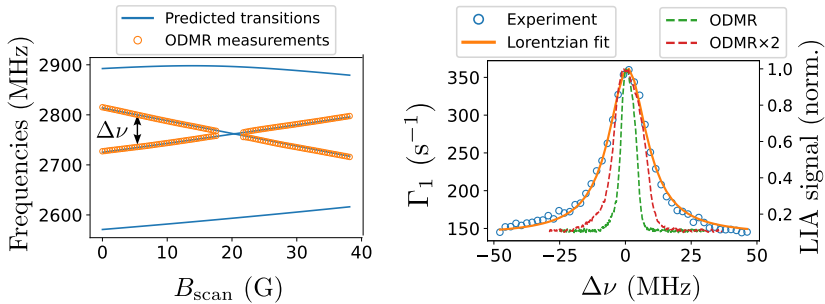
$$f(\tau) = \exp\left(-\tau/T_1^{\text{ph}} - \sqrt{\tau}/T_1^{\text{dd}}\right)$$



$$f(\tau) = \exp\left(-\tau/5 - \sqrt{\tau}/T_1^{\text{dd}}\right)$$



Fluctuator linewidth



- Γ_1 curve broader than ODMR overlap
- Lorentzian shape

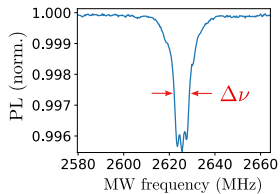


The fluctuator's spectral response (T_2^*) in broadened by γ_f

NV center magnetometry sensitivity

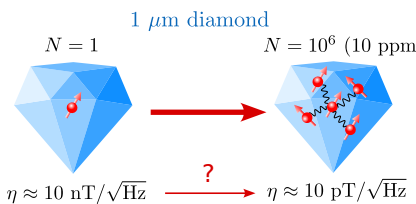
Ideal (DC) sensitivity for N independent NV centers:

$$\eta[\text{T}/\sqrt{\text{Hz}}] \approx \frac{\hbar\sqrt{\Delta\nu}}{g\mu_B C\sqrt{N}}$$

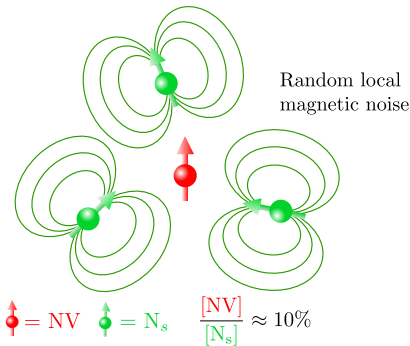


- \hbar : Planck constant
 - μ_B : Bohr magneton
 - g : NV electron Landé factor
 - C : Spin readout contrast
 - N : Number of NV centers
 - $\Delta\nu = \frac{1}{T_2^*}$: Spectral linewidth
- Constants

Experimental parameters
- Sample parameters



NV center magnetometry: the interaction limit



Going beyond the “Interaction limit” ($[\text{N}_s] > 10 \text{ ppm}$):

- Decoupling interaction (Hamiltonian engineering)
- Exploiting interactions

